18th International Conference on Structural Mechanics in Reactor Technology (SMiRT 18)
Beijing, China, August 7-12, 2005
SMiRT18-H01-4

STRUCTURE SIMULATION OF PRE-STRESSED CONCRETE CONTAINMENT STRUCTURES

Hans Grebner
GRS, Köln, Germany
Phone: 0221/2068-738, Fax: -834
E-mail: grb@grs.de

Jürgen Sievers
GRS, Köln, Germany
Phone: 0221/2068-747, Fax: -834
E-mail: siv@grs.de

ABSTRACT

With respect to the high priority of the integrity of containments for meeting safety requirements in nuclear power plants especially in the framework of probabilistic safety analyses (PSA) of level 2, the qualification of the methods, procedures and inspections used for the assessment of integrity and leak tightness is of special importance. Within a series of large scale tests on the failure behaviour of model containments a 1:4 scaled pre-stressed concrete containment model with metallic liner was investigated at Sandia National Laboratories (Albuquerque, New Mexico). After completion of the tests the International Standard Problem ISP 48, supported by CSNI/IAGE, was defined to perform an international comparative study on the present state of analysis methods used for the assessment of pre-stressed concrete containments concerning load-carrying capacity and leak tightness. Calculations were performed of the so-called Limit State Test which was finished with an internal pressure of 1.29 MPa (about 3.3 times design pressure) as well as of combined pressure and temperature loading cases. Axisymmetric and 3d finite element models were developed and used by GRS first without consideration of geometric inhomogenities due to penetrations in the wall. The steel liner at the inner surface and the concrete parts are made of continuum elements, while the rebar and tendon parts are modelled as truss elements. Nonlinear material models are used. The concrete material model includes the formation of micro-cracks for tensile stresses exceeding a critical value. In the paper selected results of GRS analyses are summarized.

Keywords: Containment, pre-stressed concrete, failure, pressure loading, thermal loading, finite elements, analysis, experiment.

1. INTRODUCTION

In France and Eastern European countries many nuclear power plants have pre-stressed containments and the European Pressurized Water Reactor (EPR) to be built in Finland will have one too. In Germany pre-stressed containments are used for the two boiling water reactors of model year 72. In the framework of German safety studies the load-carrying capacity of containment structures was estimated to identify weak spots.

Main objective of the present investigations described in the following is to further develop the structure mechanics analysis methods for the assessment of the integrity of pre-stressed concrete vessels and to improve the degree of accuracy making use of already performed large scale experiments.

 Copyright © 2005 by SMiRT18

Within the large scale test on a 1:3 scaled pre-stressed model containment with 1:1 wall thickness performed by Electricité de France (EDF) in Civeaux (Granger, Labbe, 1997) linear and nonlinear structural behaviour as well as leak rates through the concrete were investigated. The GRS calculations (Firnhaber, Sievers, Schwinges, 2000) showed that the predictive capabilities of the analysis methods with respect to the simulation of the deformation behaviour of concrete structures with inclusion of pre-stressing and rebar arrangement especially the estimation of leak openings and leak rates should be improved.

In experiments at the University of Karlsruhe (Eibl, et al., 2001) cracks were generated in large scaled concrete blocks by uniaxial tension. Then leak rate tests were performed with well defined leak openings. GRS has started to simulate the crack formation.

At SANDIA National Laboratories (Albuquerque, New Mexico) a series of large scale tests with model containments have been performed during the last 20 years. First a 1:6 scaled reinforced concrete model was investigated (Horschel, Jung, 1986). GRS has performed pre- and post-calculations of the structural behaviour of that model containment (Bachmann, et al., 1988). Then the failure behaviour of a mixed scaled steel containment was studied (Luk, et al., 2000). Recently large scale tests of the failure behaviour of a 1:4 scaled pre-stressed concrete containment model were performed. **Fig. 1** gives a schematic view of that containment model, which includes a thin metallic liner at the inner surface. A view of the completed model before the start of the experiments is shown in **Fig. 2**.

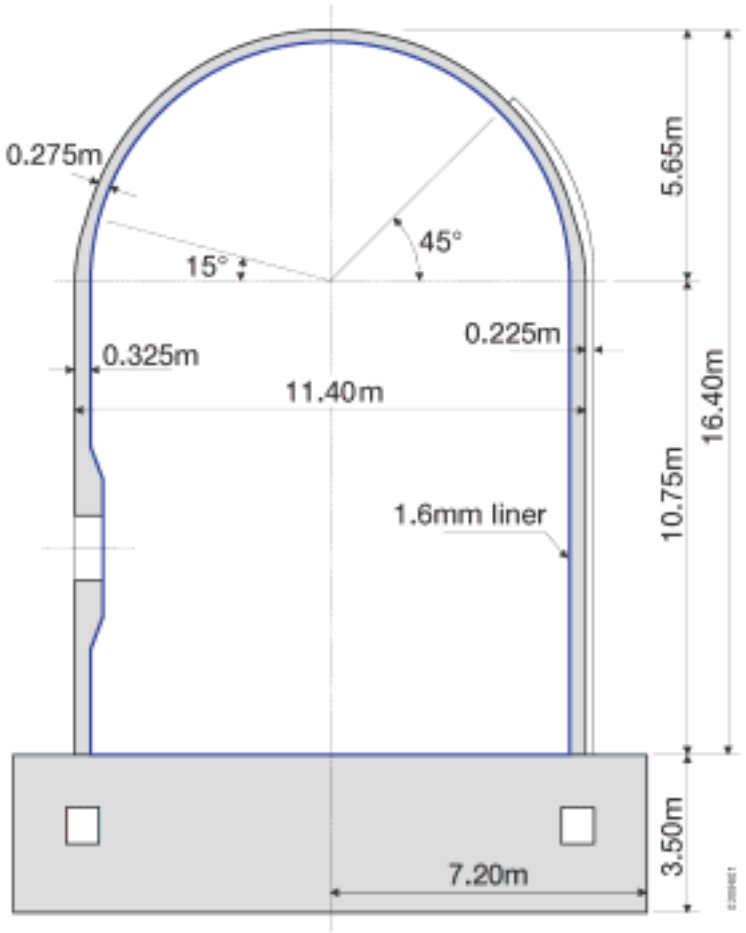

Fig. 1: Major dimensions of the pre-stressed containment model (the wall includes hoop, meridional and radial rebars as well as hoop and meridional tendons)

Copyright © 2005 by SMiRT18

Fig. 2: View of the completed Sandia containment model (from (Hessheimer, et al., 2003))

In combination with the SANDIA-Experiments pre- and posttest-calculations were carried out by several institutions. After completion of the tests the International Standard Problem (ISP) No. 48, supported by CSNI-IAGE[1] working group, was defined to perform an international comparative study on the present state of analysis methods used for the assessment of prestressed concrete containments concerning load-carrying capacity. The tasks within ISP48 include loading of the containment model by internal pressure or by superposition of pressure and temperature gradients in the wall. Especially the failure behaviour in the steel liner, the concrete and the tendons are of interest. GRS participates in ISP 48 (Grebner, Sievers, 2005). In the following selected analysis results are summarized.

Basis of the standard problem is the so-called Limit State Test (Hessheimer, et al., 2003) which was stopped at an internal pressure of 1.29 MPa (about 3.3 times design pressure). At this pressure the leak rate through leaks in the steel liner and the concrete was higher than the amount which could be compensated by the nitrogen supply system.

After repair of the liner a further test (called Structural Failure Mode Test) was performed. Before this test the model was nearly completely filled with water. The internal pressure was generated by a small amount of nitrogen. The test ended with a catastrophic failure of the containment model, as described in (Hessheimer, et al., 2003). A maximum pressure value of 1.42 MPa (about 3.63 times design pressure) was reached in this case.

[1] CSNI-IAGE: Committee on the Safety of Nuclear Installations – Integrity of Components and Structures

 Copyright © 2005 by SMiRT18

2. ANALYSIS MODELS

First axisymmetric finite element models of the 1:4 containment vessel were developed to simulate the structural behaviour without consideration of geometric inhomogenities due to penetrations in the wall. **Fig. 3** shows the analysis model and its main components.The steel liner at the inner surface and the concrete parts are made of 8-node isoparametric elements with 4 integration points, while the rebar and tendon parts are modelled as truss elements (with 3 nodes for the meridional and radial ones and one node for those in hoop direction). At the present stage a stiff coupling between steel and concrete is simulated. Dimensions and material data are taken from (Hessheimer, et al., 2003).

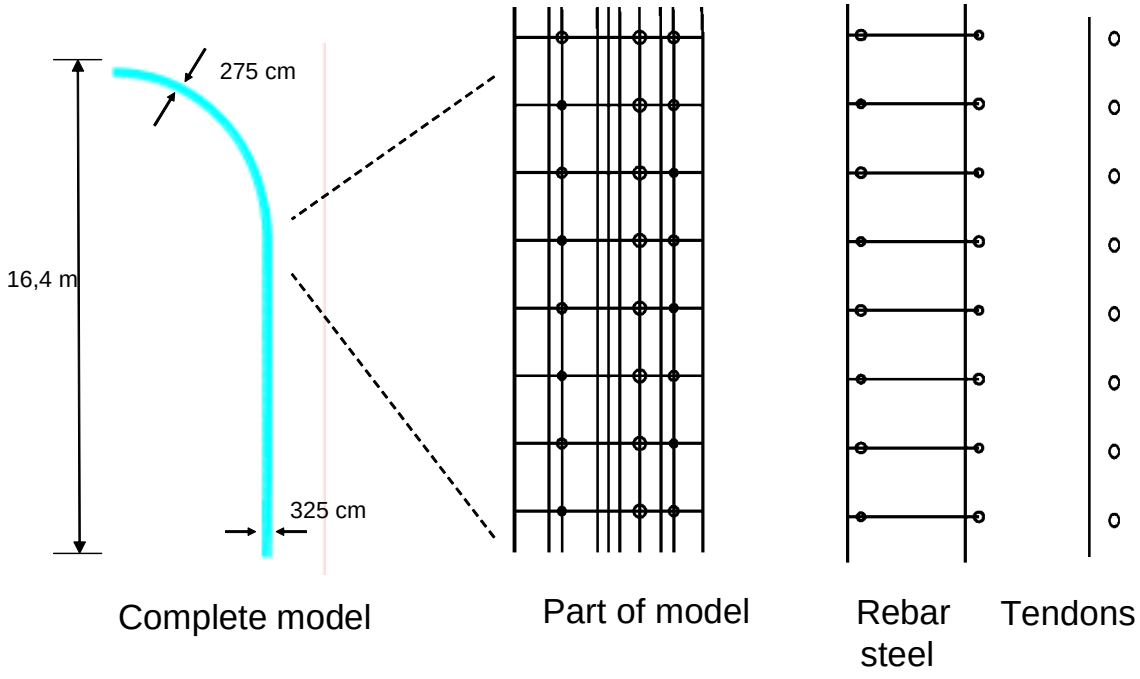

Fig. 3: Axisymmetric finite element model

During performance of the calculations with the axisymmetric model it became obvious that the dome behaviour could not be simulated well. Therefore a full three-dimensional model of a 90°-section of the containment model was developed additionally. The complete finite element model and some details are shown in **Fig. 4**. Here the position of the tendons in the dome part fully coincides with the SANDIA containment model. Again rebars and tendons are simulated by truss elements. For the concrete parts 8-node isoparametric 3d-elements are used and the liner is simulated by shell elements.

While studying a special load case with pressure and temperature loads of the ISP numerical problems showed up in calculations with the global models shown in Figs. 3 and 4. To get some local information a simple axisymmetric model (slice model) consisting of an section of the cylindrical part of the containment was considered. The model is shown in **Fig. 5**. It contains all rebar and tendon elements located in the slice.

For the liner, the rebar elements and the tendons elastic-plastic material models with temperature dependent data are used. The concrete material model includes the formation of micro-cracks for tensile stresses exceeding a critical value as well as crushing for high compressive stresses. The pre-stressing of the tendons is simulated by initial strains in the respective truss elements. The containment model is loaded by increasing internal pressure or by a combination of pressure and temperature loading. For the calculations the finite element program system ADINA (Bathe, et al., 2003) was used.

Copyright © 2005 by SMiRT18

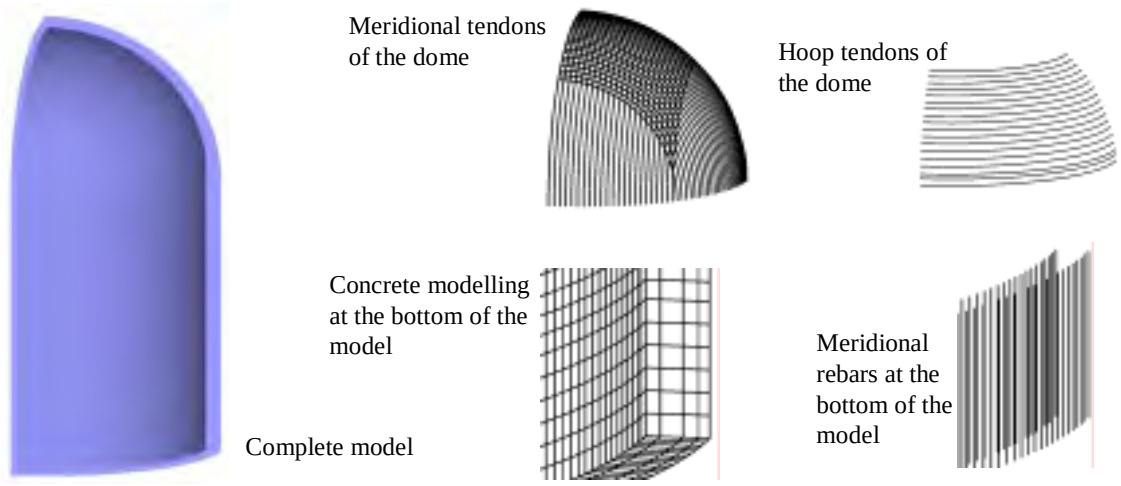

Fig. 4: 3d finite element model of a 90°-section

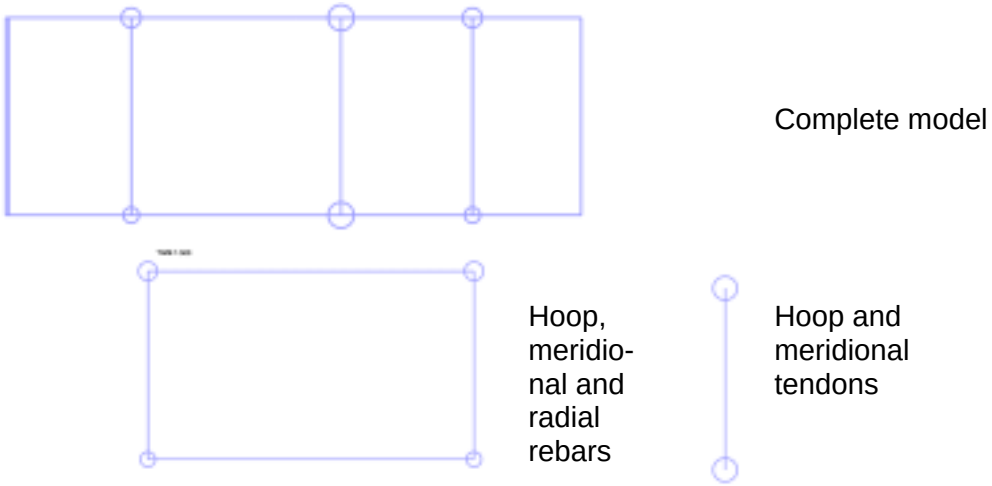

Fig. 5: Axisymmetric finite element model of a cylindrical section (slice model)

3. LOADS

As described before calculations were performed on the so-called Limit State Test with internal pressure loading (Phase 2 of ISP 48). Additionally two fictitious loading cases with a combination of internal pressure and temperature loading were considered (Phase 3 of ISP 48). In case 1 a simultaneous increase of pressure and temperature (as for saturated steam) was considered, while in case 2 a station blackout scenario is simulated. The time dependence of internal pressure and temperature at the inner surface of the containment for the two cases is shown in **Figs. 6** and **7**. Resulting temperature values are gained by heat conduction calculations with an axisymmetric model performed by David Evans and Associates (DEA) (Dameron, et al., 2004) with the temperatures of Figs. 6 and 7 as boundary conditions and are made available to the ISP participants (Hessheimer, 2004). The temperatures given at several cross sections as well as interpolated values are used as loading in the GRS calculations of the respective cases.

Copyright © 2005 by SMiRT18

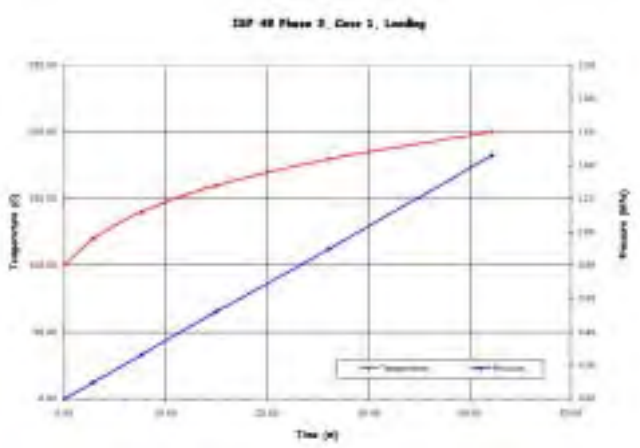

Fig. 6: Time functions for pressure and temperature at inner surface for ISP Phase 3, case 1 (from (Hessheimer, 2004))

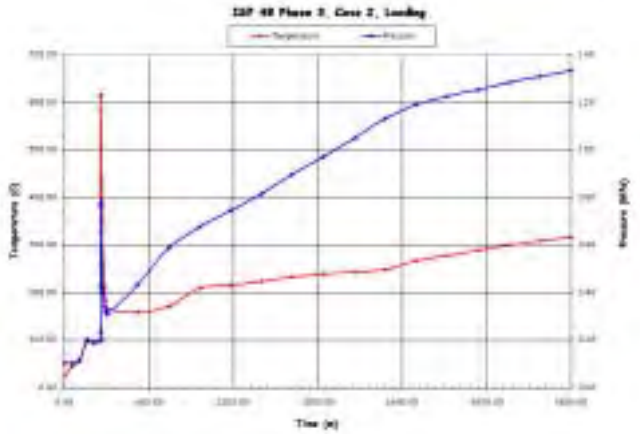

Fig. 7: Time functions for pressure and temperature at inner surface for ISP Phase 3, case 2 (from (Hessheimer, 2004))

4. ANALYSIS RESULTS

Some typical results of the different calculations are summarized in the **Figs. 8** to **21**. Analysis results of the pressure only case are presented in addition with some experimental results of the Limit State Test in chapter 4.1 and of the two pressure and temperature load cases in chapter 4.2.

4.1 Pressure only case

Figs. 8 to **11** show the deformation of the complete axisymmetric model for different values of internal pressure.

Figs. 12 and **13** present the radial displacements at 6.2 m from the basemat and the vertical displacements at the top of the dome (16.2 m) as function of internal pressure. For the vertical displacement of the top of the dome the axisymmetric model shows larger deviations to the experiment at pressure values above 0.75 MPa, while the 3d-results show a much better coincidence. This is mostly due to the more realistic modelling of the tendons in the 3d-model especially in the dome region. The axisymmetric model can not provide an adequate modelling of the hairpin tendons in the upper dome part. Furthermore the formation of micro-cracks and the post-cracking stiffening behaviour have influence on

 Copyright © 2005 by SMiRT18

the vertical deformation of the dome.

Figs. 14 and **15** give further examples of comparisons between calculations (axisymmetric and 3d) and measurement, especially strains of the rebars and tendons at typical locations in the cylindrical part of the model. Due to numerical problems at present for the 3d-calculation only results up to 1.1 MPa internal pressure are available.

For pressure loading up to 0.6 MPa (about 1.5 times design pressure) the calculated results of displacements and strain in the liner, the rebars, the tendons and the concrete agree very well with measured data. Major differences between experiment and analysis are found in the pressure region of about 0.6 to 0.74 MPa in which the crack formation in the concrete starts. The extension of micro-cracks in the slice model is presented in **Fig. 16**. The orientation of these micro-cracks is perpendicular to crack opening stresses in circumferential and axial direction. In this pressure region the deviations may be due to a too stiff coupling of concrete and steel in our finite element model, which will be investigated by further studies.

For the pressure region 0.75 to 1.0 MPa mostly a good coincidence of calculation and measurement is found. Above 1.0 MPa plastification starts in the hoop rebars and again larger differences between experiment and calculation are found. At the maximum load of the limit state test (1.29 MPa) hoop tendon strains of nearly 1% are found, which is about 30% of the uniaxial rupture strain. The maximum strain values in the rebars and the liner range below 1%. Thus a larger difference to the uniaxial rupture strain is found in this case. The structural behaviour of the cylindrical section for pressures above 1.3 MPa could be simulated only with the axisymmetric slice model. It shows increase of deformation and strains with much greater gradients due to strong plastification of the steel components. All in all it is expected that the failure of the model containment in the Structural Failure Mode Test which started with breaks of single circumferential tendons at 1.33 MPa can only be predicted by consideration of the geometric inhomogenities due to penetrations.

Fig. 8: Deformation of axisymmetric model at 0.7 MPa (magnification of displacements = 50)

Fig. 9: Deformation of axisymmetric model at 1.0 MPa (magnification of displacements = 50)

 Copyright © 2005 by SMiRT18

Fig. 10: Deformation of axisymmetric model at 1.3 MPa (magnification of displacements = 10)

Fig. 11: Deformation of axisymmetric model at 1.4 MPa (only in calculation, magnification of displacements = 10)

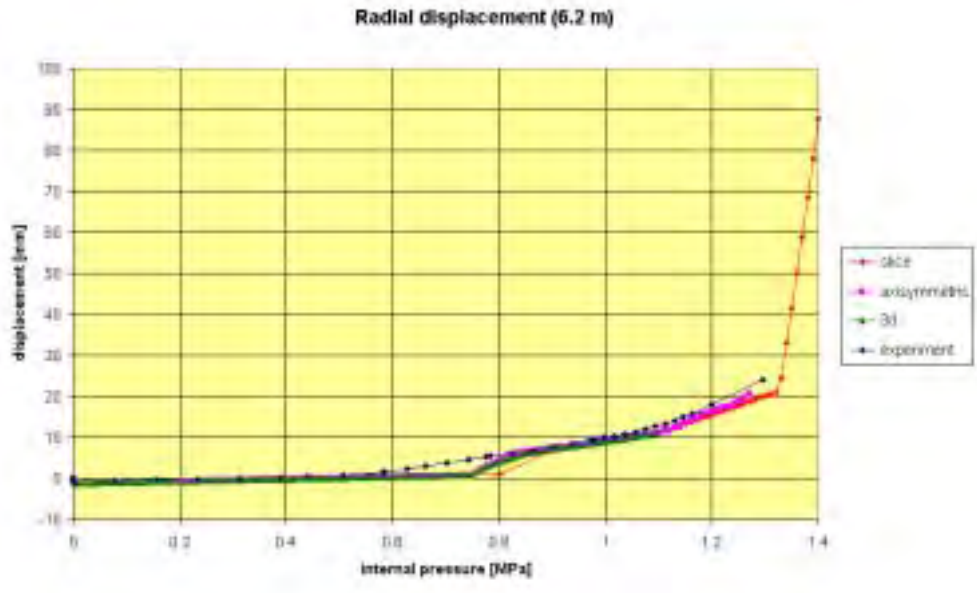

Fig. 12: Radial displacements in cylindrical containment part (position 6.2 m above basemat), pressure only – experimental values and calculated results

Copyright © 2005 by SMiRT18

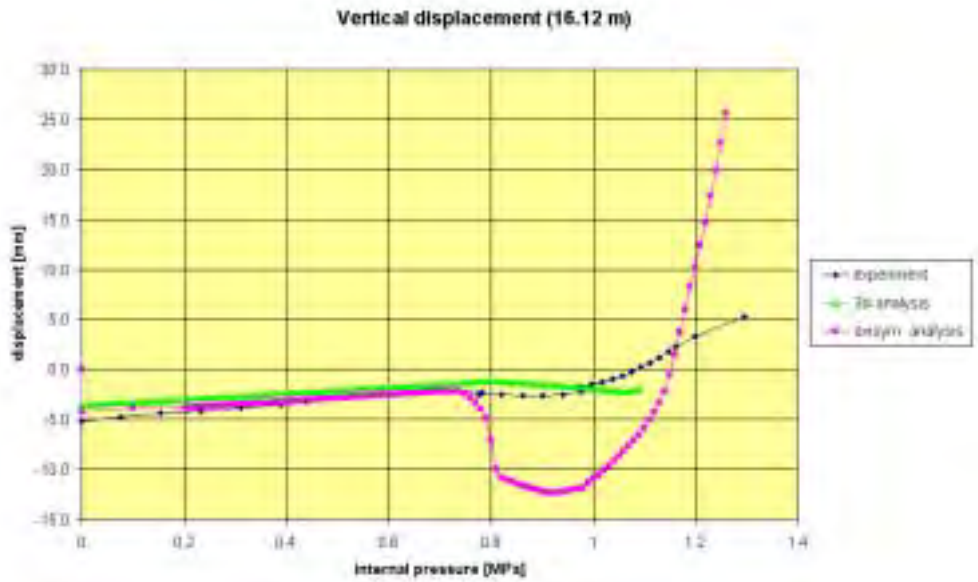

Fig. 13: Vertical displacements at top of the containment (position 16.12 m above basemat), pressure only – experimental values and calculated results

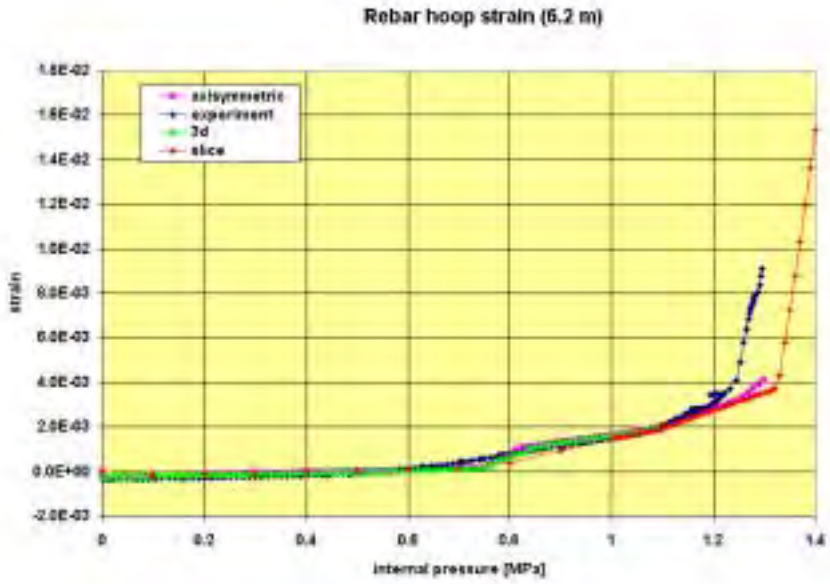

Fig. 14: Hoop rebar strains in the cylindrical part of the containment (position 6.2 m above basemat), pressure only – experimental values and calculated results

Copyright © 2005 by SMiRT18

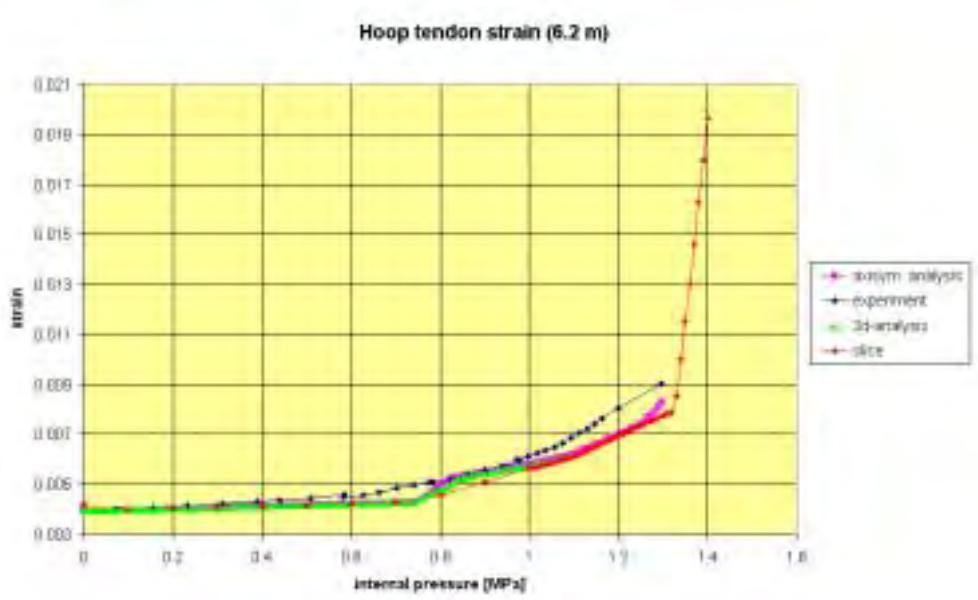

Fig. 15: Hoop tendon strains in the cylindrical part of the containment (position 6.2 m above basemat), pressure only – experimental values and calculated results

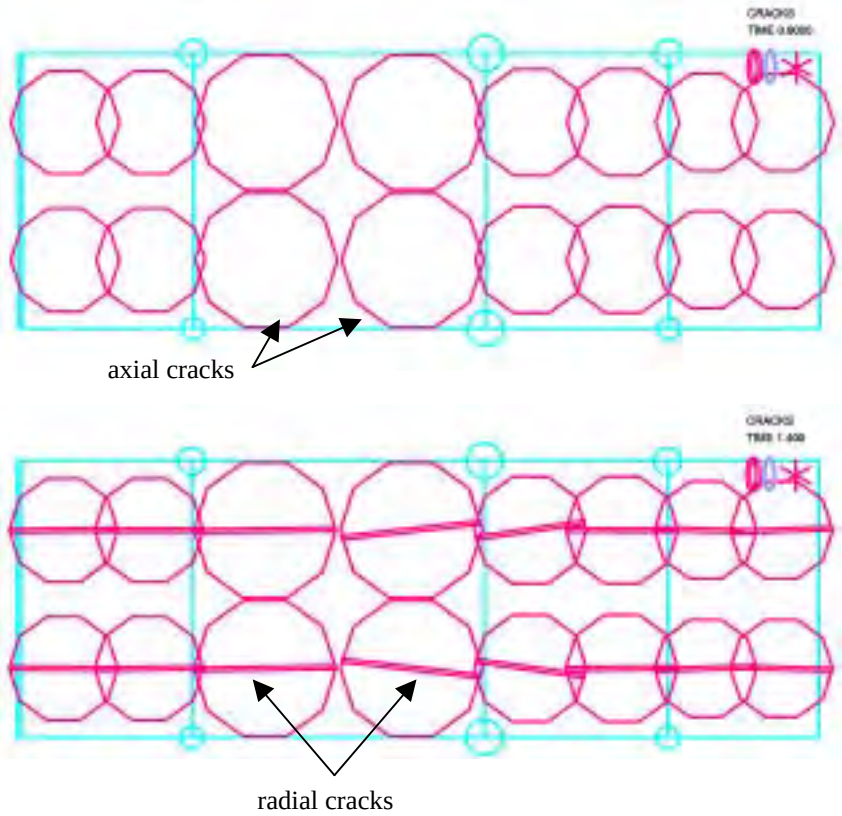

Fig. 16: Formation of axial and radial micro-cracks at internal pressures 0.8 and 1.4 MPa (axisymmetric slice model)

Copyright © 2005 by SMiRT18

4.2 Load cases with combined pressure and temperature

The next results presented are for the calculations with combined pressure and temperature loading case 1 and 2, starting with case 1.

Curves of the radial displacement are shown in **Fig. 17** for the slice model and the axisymmetric complete model (height position 6.2 m above basemat) for the case 1 temperature load compared to pressure only results for the axisymmetric complete model. The coincidence between the two models is very good, while a significant difference is found for the two load cases. **Fig. 18** shows a comparison of the hoop stress in the concrete for integration points near inner and outer wall for the slice model. The figures show that the pre-stressing of the concrete near the outer surface disappears due to the temperature gradient only, i.e. in case 1 even with internal pressure equal to zero. Due to the thermal gradient near the outside of the wall axial micro-cracks are initiated at very low pressure values, while near the inside the micro-cracks start at pressure values of about 0.7 MPa.

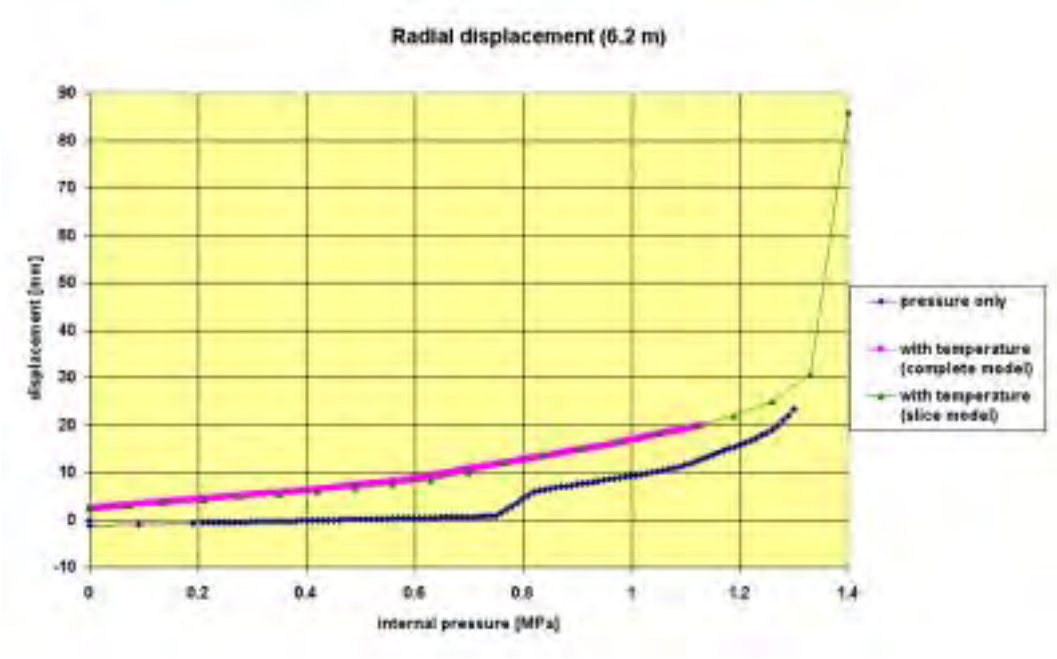

Fig. 17: Radial displacement in the cylindrical part of the containment, pressure only and temperature case 1 (complete axisymmetric and slice model)

Furthermore the behaviour of the tendons is presented in **Fig. 19**. While the meridional tendon remains elastic, the plastification in the hoop tendon starts at about 1.3 MPa. At the end of the transient, i.e. after 42 min, a strain value of about 2.7% is reached which is close to the uniaxial rupture strain.

Copyright © 2005 by SMiRT18

Fig. 18: Hoop stresses in the concrete for integration points near inner and outer wall, pressure only and temperature case 1 (slice model)

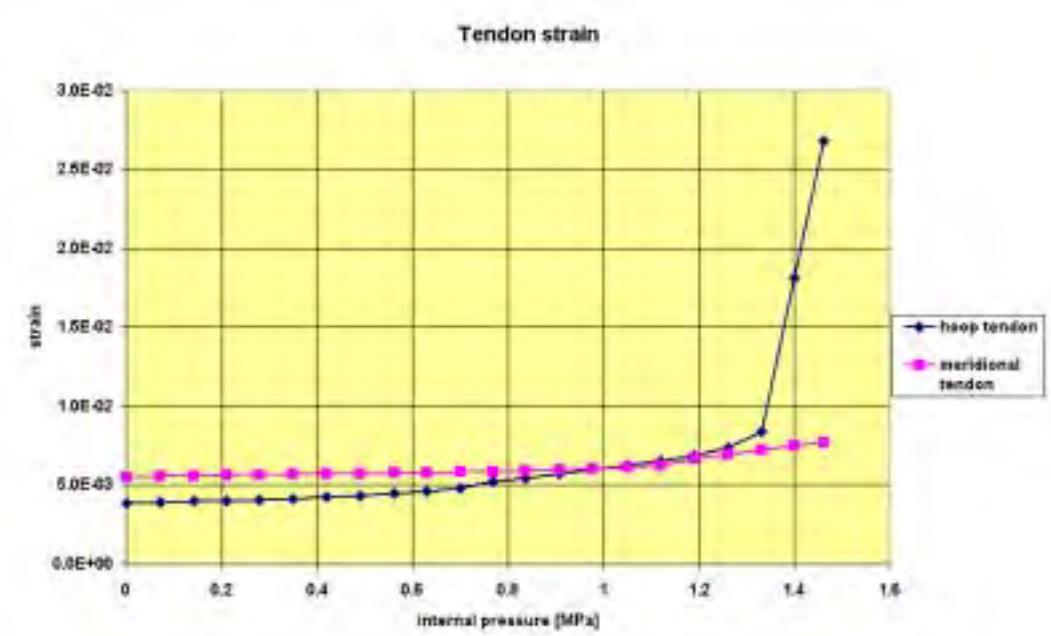

Fig. 19: Tendon strains (hoop and meridional), pressure only and temperature case 1 (slice model)

Finally selected results for case 2 are given. Due to numerical problems this load case was calculated with the slice model only, i.e. the results shown are representative for a cylindrical section at 6.2 m above the basemat. As at the inside integration point in the concrete high temperatures occur, in the first 30 hours of the transient compressive strains are found at this point. The differences obtained between inside and outside at the end of the transient are again due to the thermal gradient through the wall. **Fig. 20** shows the time dependence of the tendon strains (hoop and meridional) for two tendon trusses. The pressure and temperature peak at the begin of the transient also causes a strain peak with a maximum

 Copyright © 2005 by SMiRT18

value of about 0.75%, which is just below the beginning of plastification. Although for short times the inner surface experiences temperature values up to 600°C, at the position of the tendons (at about 58% of the wall thickness) the temperature values remain below 80°C during the whole transient. Therefore the tendons remain elastic until the end of the transient, where the hoop tendon just reaches the beginning of plastification.

Fig. 20: Tendon strains, temperature case 2 (slice model)

As in the pressure only case the calculations with temperature loading (case 1 and case 2) show regions with plastification (even at smaller pressure values). But again the maximum strain values are below the critical ones in both cases, but in case 1 the hoop tendon strains show only a small margin to the rupture strain. More details on the calculations of GRS performed within ISP 48 are presented in (Grebner, Sievers, 2005).

4.3 Crack opening displacements

If the maximum principal stress in an integration point of a concrete finite element reaches the maximum tensile stress in the concrete σ_t, a micro-crack is formed at this point according to the smeared crack approach (Bathe, et al., 2003). The stress normal to the crack surface at this point gradually decreases to zero, while the normal strain ε may be related to the crack opening displacement δ by the equation (Curbach, 1987):

$$\delta = \left(\varepsilon - \varepsilon_t\right) \cdot l_e$$

Here ε_t is the strain-value corresponding to the maximum tensile stress σ_t and l_e is a characteristic length of the element considered. If the fracture energy G_f of concrete is used as input to ADINA, l_e may be evaluated by the relation (Bathe, et al., 2003):

$$l_e = \frac{2 \cdot E_0 \cdot G_f}{\sigma_t^2 \cdot \xi}$$

E_0 is the initial Young's modulus. ξ describes the normal strain value ($\xi \cdot \varepsilon_t$), where the normal stress reaches zero. **Fig. 21** shows a typical example of the circumferential stress versus strain behaviour, calculated for the pressure only case at a concrete integration point of the slice model. If one considers a line of integration points through the containment wall, for different pressure values crack opening

 Copyright © 2005 by SMiRT18

profiles can be evaluated as presented in **Fig. 22**. At the internal pressure 1.4 MPa a crack opening displacement of nearly 0.3 mm is found through the wall.

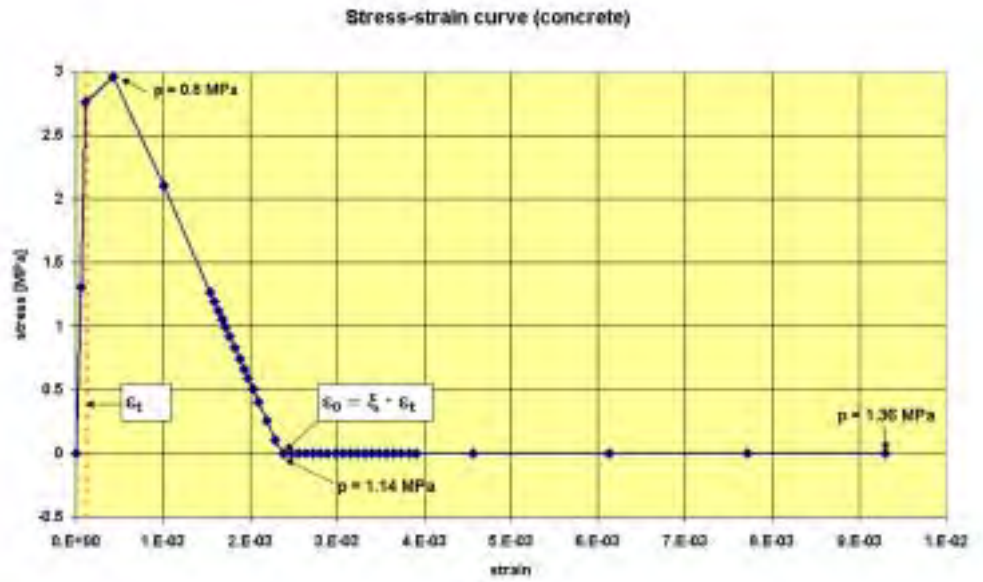

Fig. 21: Part of a typical stress-strain curve for a integration point in concrete, components normal to crack face, slice model, pressure only case

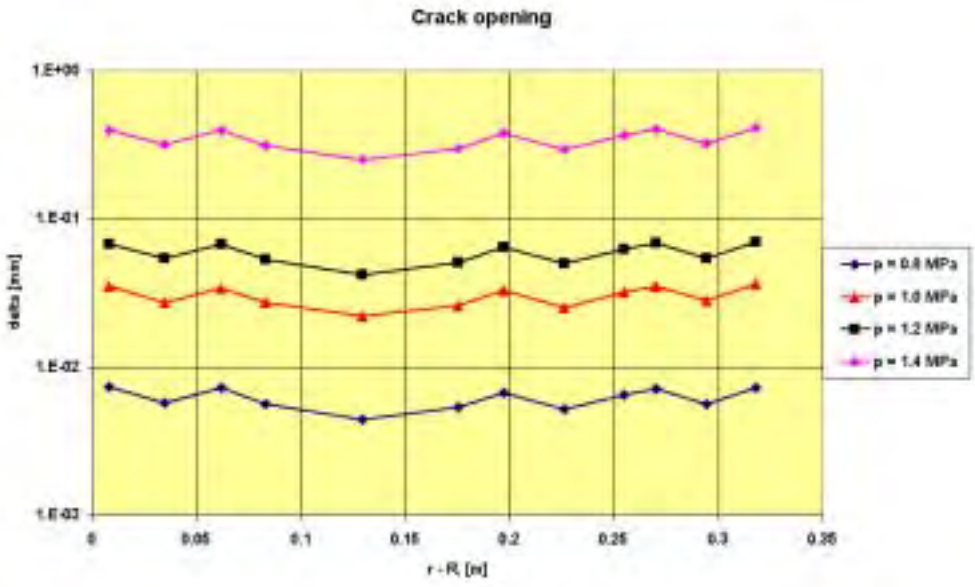

Fig. 22: Crack opening displacements for a line of integration points (in concrete) through the wall, slice model, pressure only case

To use this result for a leak rate evaluation it must be taken into account that an axisymmetric finite element model simulates one radian i.e. about 60° in circumferential direction. In the SANDIA containment model a large number of axial cracks was found for the complete circumference (Hessheimer, et al., 2003), but there is no information available about measured crack widths. Further work is necessary on that topic.

 Copyright © 2005 by SMiRT18

5. SUMMARY

The SANDIA tests of the 1:4 pre-stressed containment model of a PWR are used as basis for the validation of adequate analysis models. For this purpose axisymmetric and 3d models were developed. The concrete parts are simulated by 8-node elements, while for rebar steels and tendons truss elements are used. The metallic liner at the inside of the containment is model either by 8-node or by shell elements. The necessary input data for the non-linear material models used were deduced from data made available by SANDIA. The models are loaded by the pre-stressing of the tendons and by increasing internal pressure (up to about 1.3 MPa) as well as by additional thermal loads.

The analyses for the pressure only case show that first axial micro-cracks in the concrete are found at about 0.75 MPa and above about 0.9 MPa micro-cracks in the other directions are found. At the maximum load (1.3 MPa) almost all concrete parts of the model have micro-cracks which may cause leaks. Nevertheless the failure of the containment model is not expected for loads up to 1.3 MPa without consideration of geometric inhomogenities due to penetrations in the wall. Although the calculated strains in liner, rebars and tendons show some plastification, the maximum values are below the critical ones. The studies of the cases with temperature loading indicate that a failure of the model containment due to the combined pressure and temperature load is not expected in the regions far away from penetrations in the wall although the safety margins concerning the hoop tendon strains are relatively small. Finally first steps to estimate crack opening displacements in the concrete from the finite element results were performed.

Acknowledgement

The work described in this paper is sponsored by the German Ministry of Economics and Labor.

REFERENCES

Bachmann, P., Eisert, P., Gruner, P., Kuntze W., Schulz, H., Eibl, J., Schlüter, F.-H. (1988), Analyse zur Bestimmung des Versagensdruckes und des Versagensverhaltens eines Stahlbetoncontainments im Maßstab 1:6 (Vorausberechnungen). GRS-A-1415 .

Bathe, K. J.,et al. (2003), ADINA – A Finite-Element-Program for Automatic Dynamic Incremental Nonlinear Analysis, Version 8.1 – Theory and Modeling Guide, Volume I: ADINA. ADINA R&D, Inc..

Curbach, M. (1987), Festigkeitssteigerung von Beton bei hohen Belastungsgeschwindigkeiten. Doctor-Thesis, Karlsruhe.

Dameron, R., et al. (2004), Analysis of Axisymmetric Prestressed Concrete Containment Vessel (PCCV) Including Thermal Effects. Report David Evans and Associates, Inc., San Diego, California.

Eibl, J., et al. (2001), Untersuchungen zum Leckverhalten von Stahlbetonwänden – Leckage im Stahlbetoncontainment. Universitäten Karlsruhe und Kaiserslautern, Abschlussbericht Vorhaben 1501063 .

Firnhaber, M., Sievers, J., Schwinges, B. (2000), Berechnung des Verhaltens und der Leckrate eines Spannbetoncontainments unter schweren Störfallbedingungen. Abschlußbericht RS1093, GRS-A-2828.

Granger, L., Labbe, P. (1997), Mechanical and Leaktightness Behaviour of a Containment Mock-up Under Severe Accident. Trans. SMiRT 14, Lyon, Vol. 5, 441-448 .

Grebner, H., Sievers, J. (2005), GRS calculations in the framework of ISP48 on Sandia pre-stressed concrete containment model. CSNI Workshop on International Standard Problem 48, Lyon, April 6-7, 2005.

Hessheimer, M. F., et al. (2003), Overpressurization test of a 1:4 scale pre-stressed concrete containment model. NUREG/CR-6810.

Hessheimer, M. F. (2004), E-Mail on Temperature Gradients dated August 24, 2004.

Horschel, D. S., Jung, J. (1986), Construction and Analysis of a 1/6th-scale Concrete Containment Model.SAND 86-1089 C.

Luk, V. K., et al. (2000), Design, Instrumentation and Testing of a Steel Containment Vessel Model. NUREG/CR-5679.

 Copyright © 2005 by SMiRT18